DEVELOPMENTAL DYNAMICS 236:44–59, 2007

SPECIAL FOCUS RESEARCH ARTICLE

Gangliogenesis in the Enteric Nervous System: Roles of the Polysialylation of the Neural Cell Adhesion Molecule and Its Regulation by Bone Morphogenetic Protein-4

Christophe Faure,[1,2*†] Alcmène Chalazonitis,[2†] Catherine Rhéaume,[1] Guylaine Bouchard,[1] S.-Gopalan Sampathkumar,[3] Kevin J. Yarema,[3] and Michael D. Gershon[2]

The neural crest–derived cells that colonize the fetal bowel become patterned into two ganglionated plexuses. The hypothesis that bone morphogenetic proteins (BMPs) promote ganglionation by regulating neural cell adhesion molecule (NCAM) polysialylation was tested. Transcripts encoding the sialyltransferases, ST8Sia IV (PST) and ST8Sia II (STX), which polysialylate NCAM, were detectable in fetal rat gut by E12 but were downregulated postnatally. PSA-NCAM-immunoreactive neuron numbers, but not those of NCAM, were developmentally regulated similarly. Circular smooth muscle was transiently (E16–20) PSA-NCAM-immunoreactive when it is traversed by migrating precursors of submucosal neurons. Neurons developing in vitro from crest-derived cells immunoselected at E12 with antibodies to $p75^{NTR}$ expressed NCAM and PSA-NCAM. BMP-4 promoted neuronal NCAM polysialylation and clustering. N-butanoylmannosamine, which blocks NCAM polysialylation, but not N-propanoylmannosamine, which does not, interfered with BMP-4-induced neuronal clustering. Observations suggest that BMP signaling enhances NCAM polysialylation, which allows precursors to migrate and form ganglionic aggregates during the remodeling of the developing ENS. *Developmental Dynamics 236:44–59, 2007.* © 2006 Wiley-Liss, Inc.

Key words: NCAM, PSA-NCAM; BMP-4; GDNF; ENS development; ENS patterning

Accepted 21 June 2006

INTRODUCTION

The enteric nervous system (ENS) is the largest and most complex division of the peripheral nervous system (PNS) (Furness and Costa, 1987; Gershon et al., 1994; Gershon, 2000). The ENS is also the only region of the PNS that can mediate behaviors of organs independently of central nervous system (CNS) input. The development of the ENS is similarly complex. Precursors from vagal, sacral, and rostral truncal regions of the neural crest migrate to the bowel (Le Douarin and Teillet, 1973, 1974; Pomeranz et al., 1991; Serbedzija et al., 1991; Durbec et al., 1996; Burns and Le Douarin, 1998; Kapur, 2000), stop at appropriate locations, proliferate (Chalazonitis et al., 1998a; Heuckeroth et al., 1998), differentiate into the many different phenotypes of enteric neurons (Furness, 2000), form two ganglionated plexuses (Epstein et al., 1991; Jiang et al., 2003; Young et al., 2004a,b), and establish correct interconnections. These steps in development are dependent upon the correctly timed expression of specific transcription factors by neuronal and glia precursors

[1]Division of Gastroenterology, Sainte-Justine Hospital Research Center, University of Montreal, Montreal, Quebec, Canada
[2]Department of Anatomy and Cell Biology, Columbia University, New York, New York
[3]Whitaker Institute of Biomedical Engineering, Johns Hopkins University, Baltimore, Maryland
Grant sponsor: Sick Kids Foundation; Grant number: XG05 –026R; Grant sponsor: National Institutes of Health; Grant numbers: DK 58056 and NS15547; Grant sponsor: Sainte-Justine Hospital Research Centre (CF); Grant sponsor: Arnold and Mabel Beckman Foundation.
†Christophe Faure and Alcmène Chalazonitis contributed equally to this work.
***Correspondence to: Dr. Christophe Faure, Division of Gastroenterology, Hôpital Sainte-Justine, 3175 Chemin Côte-Ste-Catherine, Montréal (Québec), Canada H3T 1C5. E-mail: christophe.faure@umontreal.ca**

DOI 10.1002/dvdy.20943
Published online 6 September 2006 in Wiley InterScience (www.interscience.wiley.com).

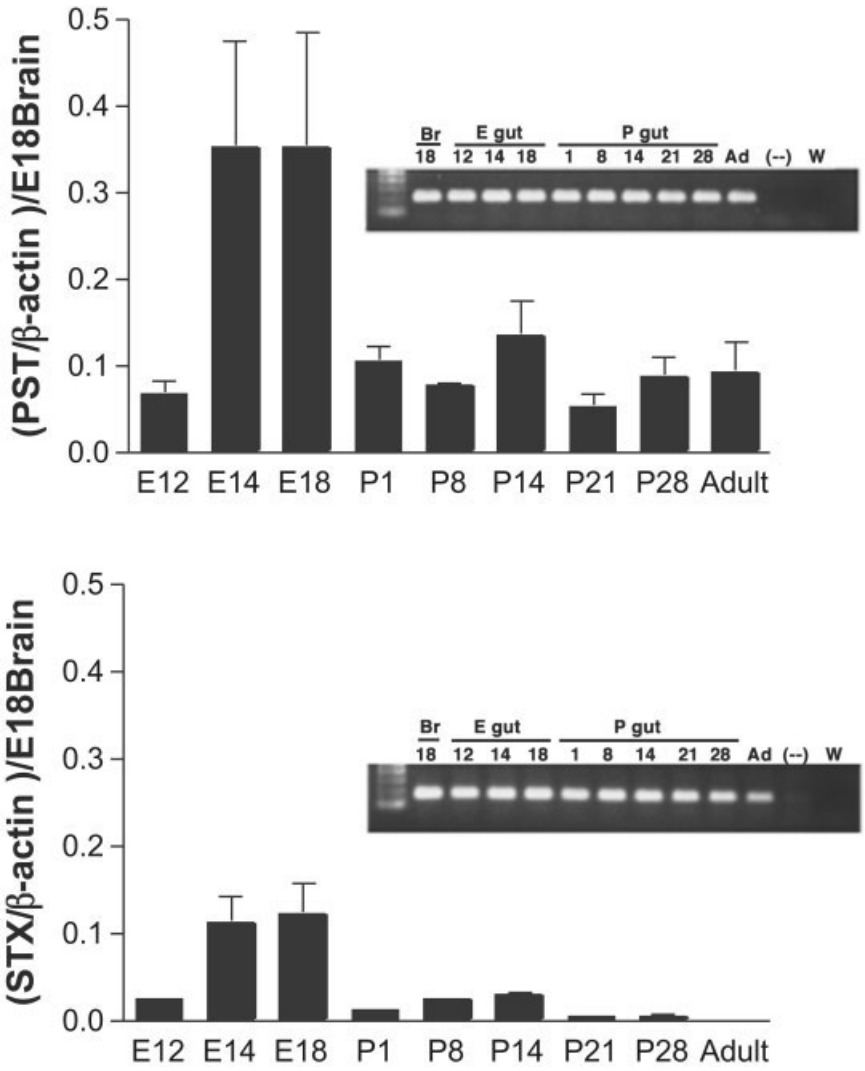

Fig. 1. Expression of PST and STX is developmentally regulated in the rat gut. Transcripts encoding PST and STX were quantified, relative to the abundance of transcripts encoding β-actin by real-time PCR. Data were normalized to the level found in the brain at E18, which was examined as a positive control. **A:** Expression of PST was detectable as early as E12, peaked at E14–E18, and declined by P1 to a low level that was maintained through adult life. **B:** Expression of STX was detectable as early as E12, peaked at E14–E18, and declined by P1 to a low level that was maintained through P14. Expression of STX declined again after P14 and was only barely detectable in the adult gut. The specificity of PST and STX primer pairs for real-time PCR was confirmed by using conventional RT-PCR followed by agarose gel electrophoresis. A single PCR band of appropriate size was obtained from each sample with each primer set (insets). DNA contamination was ruled out because no bands were obtained when reverse transcriptase was omitted and contamination was ruled out because no PCR product was obtained when the sample contained only distilled water.

and by their exposure to critical molecules provided by the microenvironment (Gershon, 2000; Newgreen and Young, 2002; Chalazonitis, 2004). These molecules include diffusible growth factors and extracellular matrix proteins. Less well studied, but probably also important are cell-to-cell and cell-to-substrate interactions, such as those mediated by adhesion molecules (Newgreen and Hartley, 1995; Araki and Milbrandt, 2000). While many of the transcription factors, growth factors, receptors, and extracellular matrix proteins that affect ENS development have been identified, relatively little is known about the role adhesion molecules play in ENS formation.

The neural cell adhesion molecule (NCAM) is a member of the immunoglobulin superfamily that functions not only in adhesive interactions, but also as a cell surface receptor (Crossin and Krushel, 2000; Paratcha et al., 2003; Rougon and Hobert, 2003). Two sialyltransferases, ST8Sia IV (PST) (Nakayama et al., 1995; Nakayama and Fukuda, 1996) and ST8Sia II (STX) (Kojima et al., 1996; Angata et al., 1997), can polysialylate NCAM (PSA-NCAM). Polysialylation reduces the adhesive properties of NCAM (Rutishauser and Landmesser, 1996), increases intermembrane repulsion (Johnson et al., 2005), and has been postulated to provide conditions that are permissive for alterations in cell position and shape (Kiss et al., 2001). PSA-NCAM has been shown to play important roles in cell migration, axonal guidance, synapse formation, and functional plasticity in the CNS (Eckhardt et al., 2000; Bruses and Rutishauser, 2001). Polysialylation of NCAM, in fact, is required during development to dampen the activity of NCAM; in the absence of polysialylation, a resulting gain in NCAM function results in severe neural defects (Weinhold et al., 2005). Whereas the expression of PSA-NCAM is high during CNS development, it is downregulated in adult life and becomes restricted to regions of the brain (Bonfanti et al., 1992) where neurogenesis persists or where cell migration, axonal outgrowth, or synaptic plasticity are ongoing (Seki and Arai, 1993; Glass et al., 1994; Lois et al., 1996; Kiss et al., 2001). NCAM is expressed in the developing ENS of humans (Romanska et al., 1996), rats (Mirsky et al., 1986; Baetge et al., 1990; Bally-Cuif et al., 1993; Newgreen and Hartley, 1995), and chicks (Akitaya and Bronner-Fraser, 1992); however, neither the function nor the regulation of enteric PSA-NCAM expression has previously been investigated.

Development of enteric neurons below the level of the esophagus depends upon stimulation of the Ret receptor tyrosine kinase (Schuchardt et al., 1994) by glial cell line–derived neurotrophic factor (GDNF) (Moore et al., 1996; Pichel et al., 1996; Sánchez et al., 1996) in a complex with GDNF family receptor α 1 (GFRα 1) (Enomoto et al., 1998). During early development, GDNF acts as a guidance molecule (Young et al., 2001, 2004a; Natarajan et al., 2002) and a mitogen (Chalazonitis

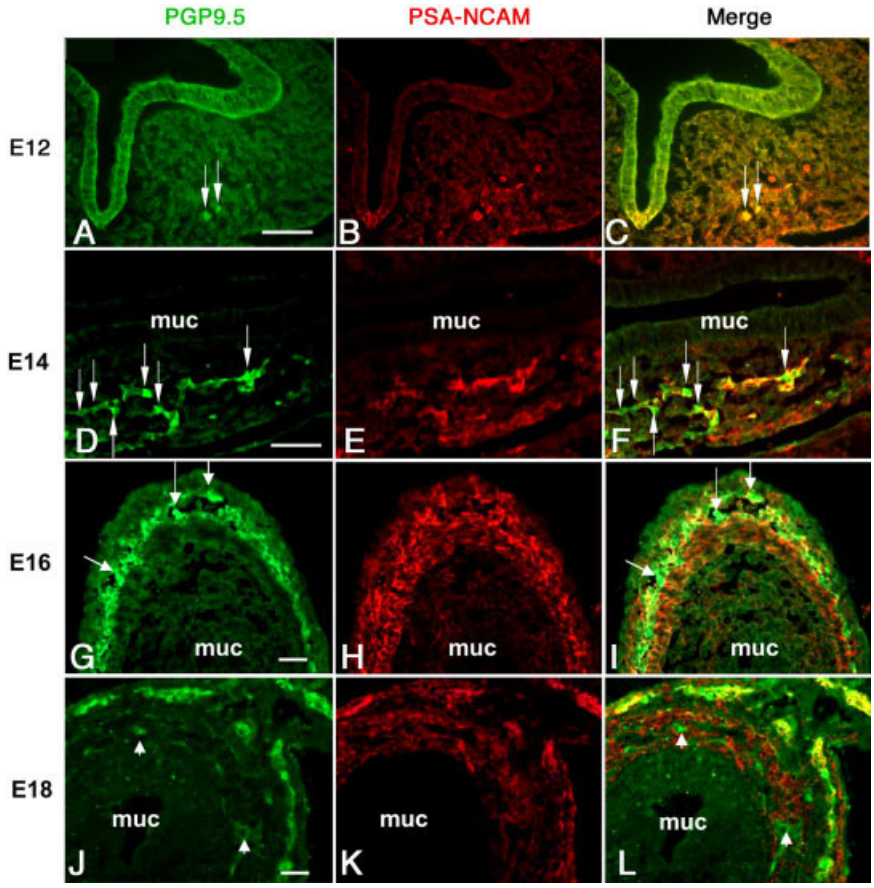

Fig. 2.

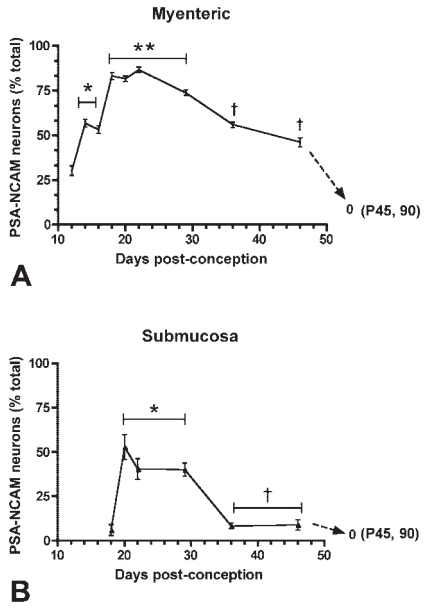

Fig. 3. The proportion of neurons in the myenteric and submucosal plexuses that displays PSA-NCAM immunoreactivity is developmentally regulated. The percent of PGP9.5-immunoreactive cells that is coincidentally PSA-NCAM-immunoreactive in each plexus was plotted as a function of days post conception (dpc). Birth occurs on day 21dpc. **A:** Myenteric plexus. *$P < 0.001$ 12dpc [E12] vs. 14 dpc [E14] or 16dpc [E16]; **$P < 0.001$ 14dpc [E14] or 16 dpc [E16] vs. 18dpc [E18], 20dpc [E20], 22dpc [P1], or 28dpc [P7]; † $P < 0.001$ 28dpc [P7] vs. 35dpc [P14] or 46dpc [P21]. **B:** Submucosal plexus. *$P < 0.001$ 18dpc [E18] vs. 20dpc [E20], 22dpc [P1], or 28dpc [P7]; †$P < 0.001$ 28dpc [P7] vs. 35dpc [P14] or 46dpc [P21].

et al., 1998a; Heuckeroth et al., 1998; Gianino et al., 2003), but later in development it loses its ability to stimulate proliferation and appears to be a trophic factor required for the maintenance of enteric neurons (Chalazonitis et al., 1998a). The proliferative expansion of the developing ENS is restricted by the effects of bone morphogenetic proteins (BMPs)-2 and -4, which oppose GDNF-induced proliferation by promoting the differentiation and specification of particular subsets of enteric neurons, such as those that express TrkC (Chalazonitis et al., 2004). BMPs-2 and -4 also induce clustering of enteric neural precursors in vitro to form ganglion-like neural aggregates (Chalazonitis et al., 2004). This effect of the BMPs suggests that they may be able to modify adhesion of enteric neural precursors to one another and/or to the substrate. If so, then it is plausible that the BMPs influence expression of an adhesion molecule, such as NCAM or PSA-NCAM. We, therefore, tested the

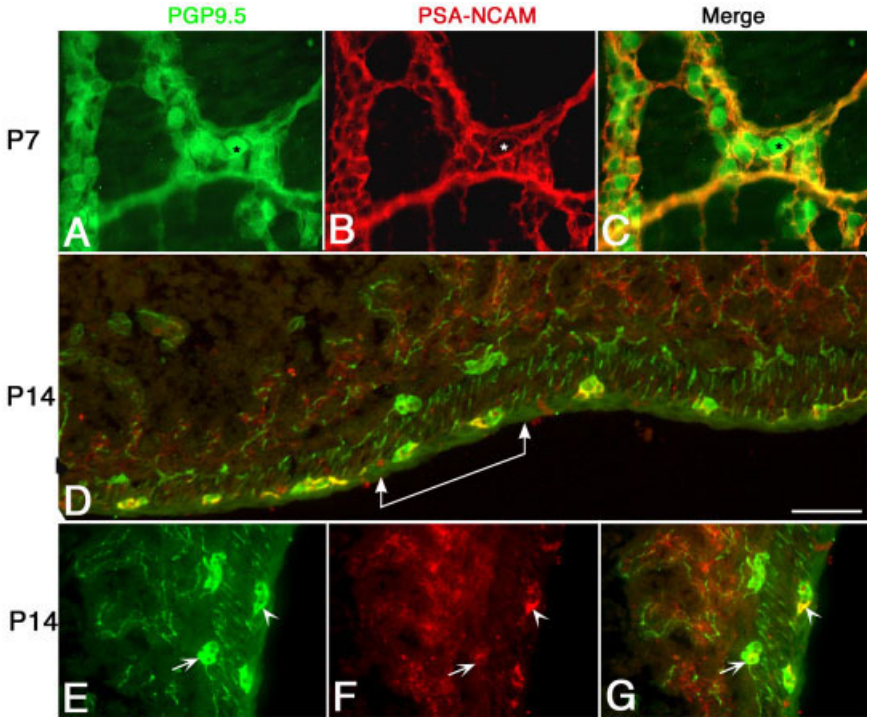

Fig. 4.

hypotheses that NCAM expression and/or its polysialylation is under BMP control and establishes conditions that favor aggregation of enteric neural precursors into the ganglia that comprise the enteric plexuses. Because enteric neurons are Ret-dependent, the response of isolated enteric neural precursors to BMPs was evaluated in the presence and absence of GDNF. Transcripts encoding the biosynthetic enzymes, STX and PST, were measured in the developing gut and PSA-NCAM expression by enteric neurons was evaluated immunocytochemically. The ability of BMP-4 to promote the polysialylation of NCAM by enteric neurons was evaluated in vitro, as was the ability of the chain terminator, N-butanoylmannosamine (ManBut) (Mahal et al., 2001) to interfere with BMP-4-induced neuronal clustering. The inactive congener, N-propanoylmannosamine (ManProp), was also investigated as a control. Data support the hypotheses that BMPs participate in sculpting the patterns of the enteric plexuses by regulating the polysialylation of NCAM. Parts of this work have previously been published in abstract form (Faure et al., 2003).

RESULTS

Enteric Expression of Transcripts of Polysialyltransferases That Add PSA to NCAM Is Developmentally Regulated

Expression of the polysialyltransferases, PST and STX, which are responsible for adding PSA to NCAM, was evaluated in the developing bowel from E12 to adult and also, as a positive control, in the E18 fetal rat brain. Transcripts encoding PST and STX were each found by RT-PCR to be expressed in the fetal rat gut from E12 through adult life (Fig. 1A,B insets). These observations are compatible with the idea that developing enteric neurons produce PSA-NCAM. Because RT-PCR is not quantitative, transcripts encoding PST and STX were also evaluated by real-time PCR (qPCR) to determine whether the expression of these enzymes is developmentally regulated (Fig. 1A,B). Expression of both PST and STX was observed to increase sharply between E12 and E14 and to be maintained through E18. Expression of PST and STX then declined between E18 and P1. Expression of PST continued at a lower level during postnatal life while that of STX was almost completely downregulated in the gut of adult animals. These data are compatible with the idea that polysialylation of NCAM is physiologically most significant during the period of late fetal life when enteric ganglia become organized (Epstein et al., 1991; Tanano et al., 2005).

PSA-NCAM Expression Is Developmentally Regulated

Enteric neurons.

Immunostaining with antibodies to PGP9.5 was used to identify cells committed to a neuronal lineage in the developing gut. PSA-NCAM immunoreactivity was visualized simultaneously by double-label immunocytochemistry. Coincident labeling of cells by antibodies to PSA-NCAM and PGP9.5 indicated that neurons express PSA-NCAM in the primordial myenteric plexus as early as E12, the youngest age examined (Figs. 2A–C, 3A). Myenteric PGP9.5-immunoreactive cells became more abundant at E14 and the proportion that were doubly-immunostained with PSA-NCAM antibodies increased significantly (Figs. 2D–F, 3A). This proportion increased again after E16 (Figs. 2G–I, 3A) to reach a peak at E18 (Fig. 2J–L) that was maintained through P7 (Fig. 3A). At E16, the developing circular layer of smooth muscle was visible and also displayed significant PSA-NCAM immunoreactivity (Fig. 2H,I). No PGP9.5-immunoreactive cells were detected in the fused mucosa-submucosal layer at E12–16; the earliest rudiments of a submucosal plexus appeared at E18 (Fig. 2J). At this time, about 10% of the PGP9.5-immunoreactive cells in the submucosal layer displayed coincident PSA-NCAM immunoreactivity (Figs. 2J–L, 3B); this proportion increased significantly at E20 (Fig. 3B). PSA-NCAM immunoreactivity continued to be expressed in subsets of PGP9.5-immunoreactive cells in both myenteric and submucosal layers through the end of prenatal life at E20 (not illustrated).

Overall, about 30% of the PGP9.5-immunoreactive cells in the myenteric layer co-expressed PSA-NCAM at E12; this proportion increased to 50% at E14 and E16 (Fig. 3A) and then

Fig. 2. PSA-NCAM is partially co-expressed with the neuronal marker PGP9.5 in the developing mid gut. **A–C:** E12. Developing neurons (A, arrows), which are scattered in the outer gut mesenchyme, coexpress PSA-NCAM (B). The arrows in the merged image (C) highlight the yellow fluorescence of the doubly labeled neurons. **D–F:** E14. Antibodies to PGP9.5 and PSA-NCAM doubly label many neurons. A subset of neurons (arrows in D and F) does not co-express PSA-NCAM. Note that developing neurons are found in chains of cells. **G–I:** E16. Antibodies to PGP9.5 and PSA-NCAM still doubly label many neurons; however, a subset of neurons (arrows in G and I) still does not co-express PSA-NCAM. The mesenchyme immediately internal to the neurons in the region of the primordial circular muscle layer has now acquired PSA-NCAM immunoreactivity and does not overlap with the neuronal layer (see particularly the merged image in I). **J–L:** E18. Antibodies to PSA-NCAM doubly label almost all neurons in the myenteric plexus (compare J with L), ganglia of which have now become evident. The region of the developing circular muscle also contains PSA-NCAM immunoreactivity. Two neurons internal to the circular muscle are indicated (arrows, J and L) signaling the initial formation of the submucosal plexus. muc, mucosa. Scale bars = 25 μm.

Fig. 4. PSA-NCAM immunoreactivity is present postnatally. **A–C:** Dissected whole mount of the myenteric plexus at P7 [28dpc]. PGP9.5 immunoreactivity (A), PSA-NCAM immunoreactivity (B), merged image (C; double labeling appears yellow). PSA-NCAM immunoreactivity outlines nerve cell bodies (*), consistent with a location in their plasma membranes, and is intense in interganglionic connectives. **D–G:** Sections of gut wall at P14 [35dpc]. The region between the arrows in the large merged image (D) has been rotated 90° and is shown in E–G. These panels were illuminated to show the individual immunoreactivities of PGP9.5 (E) and PSA-NCAM immunoreactivity (F), which also were merged (G). Submucosal ganglia can be seen as a distinct layer internal to the circular muscle, which no longer displays significant PSA-NCAM immunoreactivity. The proportion of doubly labeled neurons in the myenteric plexus (arrowhead) has begun to decrease. Only occasional submucosal neurons are PSA-NCAM immunoreactive (arrow). The red fluorescence in the lamina propria of the mucosa (seen in F and G) is non-specific. Scale bar = 80 μm.

increased significantly again to about 80% at E18–E20. The proportion of myenteric neurons that displayed PSA-NCAM immunoreactivity declined gradually during postnatal life, reaching a level by P14 that was not significantly different from that at E14–16 (Figs. 3A, 4). By P14, the mature form of the ENS had been achieved, with well-formed myenteric and submucosal plexuses (Fig. 4). At this time, although relatively little PSA-NCAM immunoreactivity remained in nerve cell bodies, axons were still PSA-NCAM immunoreactive and formed rings around the non-immunoreactive neurons (Fig. 4). At P32, PSA-NCAM-expressing neurons were rare (Fig. 5A–F) and by P45,they were no longer found in the myenteric plexus (Fig. 5G–I). At P32, PSA-NCAM expression persisted in interganglionic connectives of the myenteric plexus to a greater extent than in ganglia (Fig. 5D–F). About 50% of PGP9.5-immunoreactive cells in the submucosal layer were PSA-NCAM-immunoreactive at E18–20, when such cells were most prevalent (Fig. 3B). The proportion of submucosal neurons expressing PSA-NCAM remained relatively level through P7 but then declined significantly to <10% at P14 where it remained through P24 (Figs. 3B, 5A–C). As in myenteric ganglia, by P45, PSA-NCAM-expressing neurons were no longer found in the submucosal plexus (Fig. 5G–I). No differences were seen between the foregut, the midgut, and the hindgut in the proportions of PGP9.5-immunoreactive cells co-expressing PSA-NCAM immunoreactivity in either the myenteric or submucosal layers.

Non-neuronal cells of the enteric mesenchyme.

PSA-NCAM immunoreactivity was found in non-neuronal cells of the enteric mesenchyme as well as in the developing enteric plexuses (Figs. 2, 6). An antibody to desmin was used to test the hypothesis that these non-neuronal PSA-NCAM-immunoreactive mesenchymal cells were in the muscle lineage. Coincident desmin and PSA-NCAM immunostaining was observed in cells of the intestinal mesenchyme (Fig. 6). Although such cells were seen at E14,

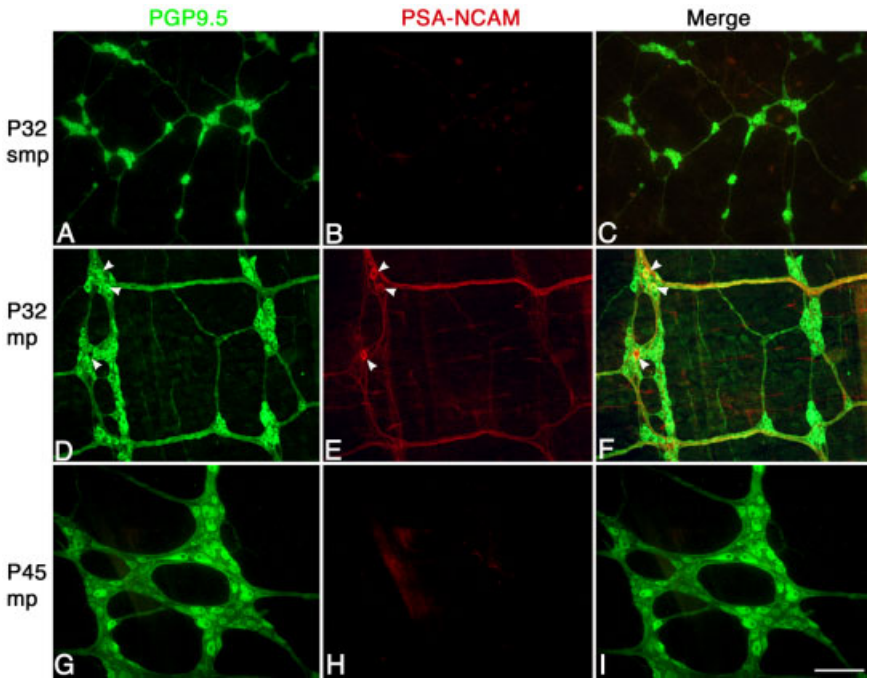

Fig. 5.

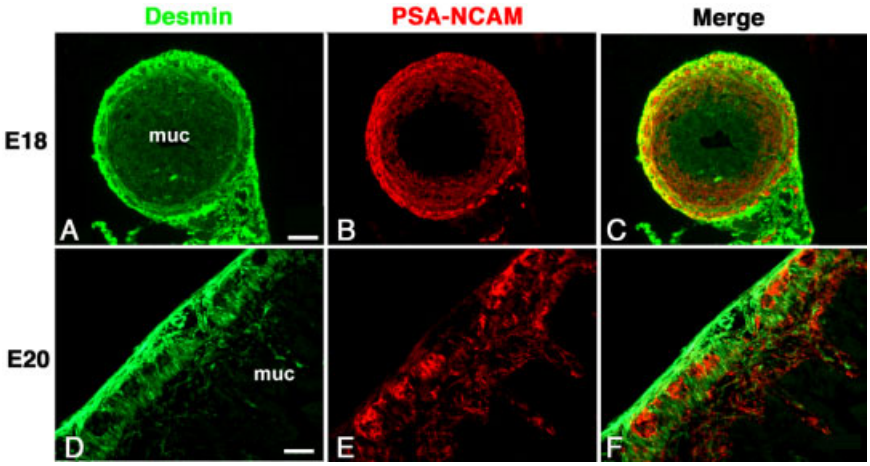

Fig. 6.

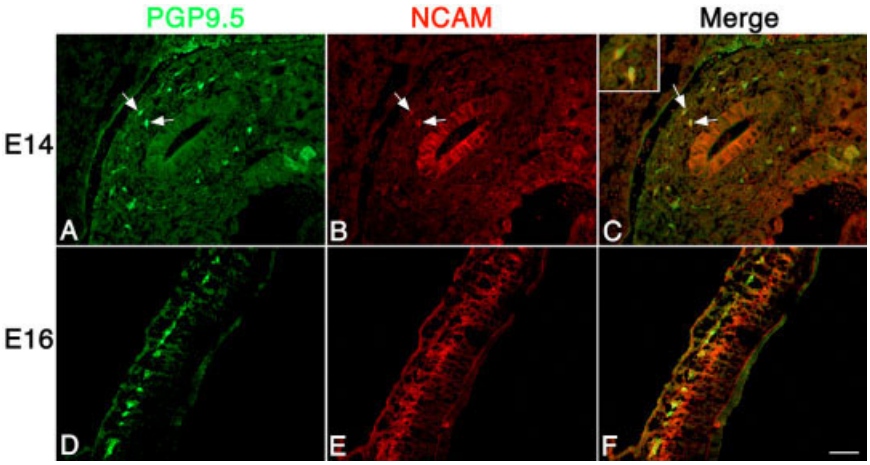

Fig. 7.

they did not exhibit a well-organized pattern. By E18, however, both the longitudinal and circular layers of smooth muscle displayed coincident desmin and PSA-NCAM immunoreactivities (Fig. 6A–C). PSA-NCAM largely disappeared from the muscle layers at E20 (Fig. 6D–F). No expression of PSA-NCAM is found in post-natal intestinal smooth muscle.

NCAM Expression Is Not Developmentally Regulated

During fetal life E12–20, NCAM immunoreactivity was present both on cells committed to a neuronal lineage (Fig. 7A–F), which were identified by their PGP9.5-immunoreactivity, and on non-neuronal cells of the enteric mesenchyme (Fig. 7E,F). NCAM immunoreactivity appeared earlier in the neuronal lineage and was co-localized with PGP9.5 at E12–E14. The non-neuronal NCAM immunoreactivity was evident in the developing circular muscle layer at E16 (Fig. 7E,F). NCAM immunoreactivity continued to be present and co-localize with PGP9.5 in both the submucosal (Fig. 8A–C) and myenteric (Fig. 8D–F) plexuses in young animals through weaning and in adults, suggesting that the lack of PSA-NCAM expression in neurons at these ages is due to a down-regulation of the polysialylation of NCAM and not to a down-regulation of NCAM expression itself. On the other hand, NCAM expression in post-natal animals did not appear to be neuron-specific; NCAM immunoreactivity was also coincident in these animals with that of S-100β, a glial marker (not illustrated). In contrast to its persistence in the enteric plexuses, NCAM immunoreactivity disappeared from the non-neuronal cells of the smooth muscle layers of the postnatal bowel.

NCAM-Immunoreactive Neurons Develop From Crest-Derived Precursors In Vitro

Experiments were carried out to test the hypotheses that the ability of BMP-4 to promote the differentiation of enteric neurons enhances the polysialylation of NCAM and enables these cells to migrate toward one another and form aggregates. Crest-derived cells were isolated from the fetal rat gut at E12 by immunoselection with antibodies to $p75^{NTR}$ (Chalazonitis et al., 2004). The cells were then cultured in defined media and exposed to BMP-4. Cells were exposed to low (0.5 ng/ml) or high (50.0 ng/ml) concentrations of BMP-4 and responses were evaluated after 2, 4, and 6 days of exposure in order to evaluate the concentration-effect and time-action relationships. Cultures were grown ± GDNF because GDNF is an essential factor for the development and maintenance of enteric neurons. Controls were exposed either to vehicle or to GDNF in the absence of BMP-4.

NCAM-immunoreactive cells developed in all of the cultures of immunoselected crest-derived cells (Fig. 9). Most of these cells were also Hu-immunoreactive and thus were neurons; however, a small proportion ($12 \pm 4\%$; $n = 9$; $P < 0.01$) of NCAM immunoreactive cells under all experimental conditions lacked Hu immunoreactivity (Fig. 9A–C). These NCAM+/Hu− cells were evidently still proliferating and thus could be seen to be dividing (insets, Fig. 9A–C). NCAM+/Hu− cells are likely to be precursors. The proportion of neurons expressing NCAM did not change significantly as a function of time when cells were cultured in the presence of BMP-4 or GDNF. In contrast, when cells were exposed only to vehicle, the proportion of neurons displaying NCAM immunoreactivity declined in a linear time-related fashion (slope = -7.2 ± 0.5; $r^2 = 0.99$; $P < 0.05$). BMP-4 and GDNF have previously been shown to promote both the development of neurons and their aggregation (Chalazonitis et al., 1998a, 2004). As expected, therefore, the size and number of neuronal aggregates were increased by exposure to BMP-4 ± GDNF (compare Fig. 9D–I to Fig. 9A–C). The neuronal aggregates tended to be larger and neuronal processes were more abundant when cells were exposed to a high concentration of BMP-4 in the presence of GDNF (compare Fig. 9D–F to 9G–I). The number of NCAM-immunoreactive cells, like the number of neurons, was also increased after 2 days of exposure to BMP-4 ± GDNF (to $847 \pm 170\%$ of vehicle; $P < 0.03$). After longer exposures to BMP-4, however, even in the presence of GDNF, the number of NCAM-immunoreactive cells declined, like that of neurons (Chalazonitis et al., 2004), and was not significantly different from vehicle-exposed cells after 6 days.

BMP-4 Promotes the Polysialylation of Neuronal NCAM In Vitro

Although BMP-4 did not alter the proportion of neurons expressing NCAM, BMP-4 significantly increased the proportion of neurons that expressed PSA-NCAM (Fig. 10A,C–E). This ef-

Fig. 5. PSA-NCAM immunoreactivity disappears from mature ganglia in both plexuses. **A–C:** P32 [53dpc] Whole mount of the submucosal plexus (smp) of the small intestine. The definitive pattern of ganglia and connectives has been achieved, but neither exhibit PSA-NCAM immunoreactivity. **D–F:** P32 [53dpc] Whole mount of the myenteric plexus (mp) of the small intestine. The definitive pattern of ganglia and connectives has been achieved. PSA-NCAM immunoreactivity is limited to a minority of nerve cell bodies (arrowheads), but is still prominent in the neurites within the interganglionic connectives. **G–I:** P45 [66dpc] Whole mount of the myenteric plexus of the colon. The definitive pattern of ganglia and connectives is evident; however, PSA-NCAM immunoreactivity is apparent neither in nerve cell bodies nor in interganglionic connectives. Scale bar = 100 μm.

Fig. 6. The circular layer of smooth muscle transiently expresses PSA-NCAM immunoreactivity. **A–C:** E18 midgut. The gut is ringed by desmin immunoreactivity (A). Coincident labelling by antibodies to desmin and PSA-NCAM occurs (B, C); the ganglia that lack desmin appear as negative images in A and stand out as red fluorescent islands within the co-labeled muscle in C. **D–F:** E20 midgut. The smooth muscle now displays only desmin immunoreactivity (D) and lacks that of PSA-NCAM (E, F). Scale bars = 40 μm.

Fig. 7. Enteric neurons are NCAM-immunoreactive in the fetal gut. **A–C:** E14 midgut. The immunoreactivity of the neuronal marker PGP9.5 (A) and that of NCAM (B) are coincident (merged image). The bright staining of the endoderm in B is inconsistent and is non-specific. The arrows indicate co-labeled neurons (shown at higher magnification) in the inset in C. **D–F:** E16. The gut now contains many more PGP9.5-immunoreactive neurons (D), which appear in a coherent chain in the outer gut mesenchyme. NCAM immunoreactivity (E) is found in the neurons, where it co-localizes with that of PGP9.5 (F; yellow fluorescence), but it is also found internal to the neurons in the developing circular layer of smooth muscle (F; red fluorescence). Scale bar = 100 μm.

fect was time-dependent and was not significantly affected by the presence of GDNF (Fig. 10B). The promotion of the sialylation of NCAM was similar for low and high concentrations of BMP-4 (Fig. 10A) and independent of GDNF (Fig. 10B). In contrast, the proportion of neurons expressing PSA-NCAM declined as a function of time in cultures exposed only to vehicle (Fig. 10A,F–G) or only to GDNF (Fig. 10B). After 6 days of culture in BMP-4 ± GDNF, PSA-NCAM expression was abundant both on nerve cell bodies and neurites (Fig. 10C–E), but was sparse and mainly on neurites when cultures were exposed only to vehicle (Fig. 10F–H).

BMP-4 Enhances Neuronal Clustering

As reported previously (Chalazonitis et al., 2004), exposure to BMP-4 promoted the clustering of neurons. The sizes of individual neuronal clusters varied and were categorized as medium (11–20), large (21–30), or extra large ≥ 31). Small groups of loosely packed neurons (<10 cells) occurred in all cultures, were unaffected by BMP-4, and could have occurred as a result of chance. The numbers of neurons in clusters of 11 or more cells were thus quantified as a function of time in culture, as were the total numbers of neurons in each culture. Significant clustering (formation of clusters of >11 neurons) of neurons was detected after 2 days in culture in the presence of BMP-4 ($P < 0.05$) and, if GDNF was present, clustering persisted for 6 days (Fig. 11A; $P < 0.001$ vs. vehicle). When cells were cultured in the presence of BMP-4 (50 ng/ml), but in the absence of GDNF, the numbers of neurons in clusters was maximal after 4 days in vitro but then declined at day 6 to a value that was not significantly different from that of vehicle-exposed cells (Fig. 11A). The total number of neurons, however, also declined (because BMP-4 promotes apoptosis) as a function of time when crest-derived precursors were exposed to BMP-4 (50 ng/ml) (Chalazonitis et al., 2004). As a result, when normalized to the total number of neurons in each culture, the proportion of neurons in clusters remained high between days 4 and 6 in vitro (Fig. 11B; $P < 0.01$ vs. vehicle). The apparent decline in numbers of neurons in clusters was prevented when cells were exposed to GDNF (10 ng/ml) as well as to BMP-4 (Fig. 11A; $P < 0.001$ vs. vehicle or BMP-4 alone). Under these conditions, the numbers of neurons in clusters (Fig. 11A) increased significantly ($P < 0.001$) between days 4 and 6, although there was not a similar increment in the proportion of total neurons that were clustered (Fig. 11B). GDNF thus does not appear to enhance the cluster-promoting effect of BMP-4 although it prevents the BMP-4-induced decrease in neuronal numbers. The proportion of neurons in clusters was correlated with the proportion of neurons expressing PSA-NCAM (Fig. 11C). Neuronal clustering and PSA-NCAM expression were both enhanced by exposure to BMP-4 ± GDNF. GDNF alone increased the proportion of neurons in clusters after 6 days in culture (7.8- ± 3.9-fold vehicle); however, in contrast to BMP4, GDNF did not increase the proportion of neurons expressing PSA-NCAM (1.1- ± 0.5-fold vehicle).

ManBut Specifically Antagonizes BMP-4-Induced Neuronal Clustering

Immunoselected crest-derived cells were cultured for 5 days, as described above, in the presence of BMP-4 + GDNF to induce neuronal clustering. After one day in vitro, cultures were exposed to vehicle (control), the chain terminator, ManBut (5 mM), to inhibit the polysialylation of NCAM, or to the inactive congener, ManProp (5 mM). Clustering was quantified as described above. Neurons were considered to be clustered if they were found in groups of >11. Smaller clusters (4–10 neurons) were also quantified, but the appearance of these aggregates was, as noted above, independent of BMP-4. PGP9.5 immunoreactivity and PSA-NCAM were demonstrated and used to visualize neurons and evaluate their status of polysialylation of NCAM (Fig. 12). The clustering of neurons induced by BMP-4 (Figs. 12A,G, 13A) was significantly inhibited by ManBut (Figs. 12D,M, 13A) but was unaffected by the addition of ManProp (Figs. 12J, 13A). ManBut (Fig. 12E,F [compare to B,C], N,O [compare to H,I]), but not ManProp (Fig. 12K,L [compare to H,I]) also decreased the polysialylation of NCAM. The BMP-4-independent formation of small aggregates of neurons was not affected by ManBut or ManProp (data not illustrated). In contrast to its effects on neuronal clustering and the formation of PSA-NCAM by cultured enteric neurons, ManBut did not alter neuronal survival; therefore, no significant differences were found in the total number of neurons in cultures exposed to BMP-4 + GDNF supplemented by vehicle, ManBut, or ManProp (Fig. 13B). ManBut thus inhibited the formation of PSA-NCAM by enteric neurons in vitro and this inhibition was accompanied by a loss of BMP-4-induced clustering. The effects of ManBut, moreover, were specific because they were not shared by ManProp and because they occur without altering neuronal survival.

DISCUSSION

The current experiments tested the hypotheses that the polysialylation of NCAM expressed by enteric neurons is promoted by BMP signaling and establishes conditions that are essential for the formation of enteric ganglia. Prior studies had demonstrated that enteric neurons and their precursors do indeed express NCAM (Baetge et al., 1990; Newgreen and Hartley, 1995), but these earlier investigations did not focus on the formation of PSA-NCAM. We now show that both of the enzymes that polysialylate NCAM, STX (Kojima et al., 1996; Angata et al., 1997) and PST (Nakayama et al., 1995, 1998; Nakayama and Fukuda, 1996), are expressed in the developing bowel; moreover, the enteric expression of these enzymes is developmentally regulated. Real time RT-PCR revealed that transcripts encoding STX and PST are both most abundant between E14 and E18. Expression of each declines in postnatal life, although PST expression persists in adult gut, while that of STX does not. The temporal regulation of STX and PST in the gut is similar to that described previously for the brain, in that STX predominates during development, while PST persists in the adult brain in regions associated with

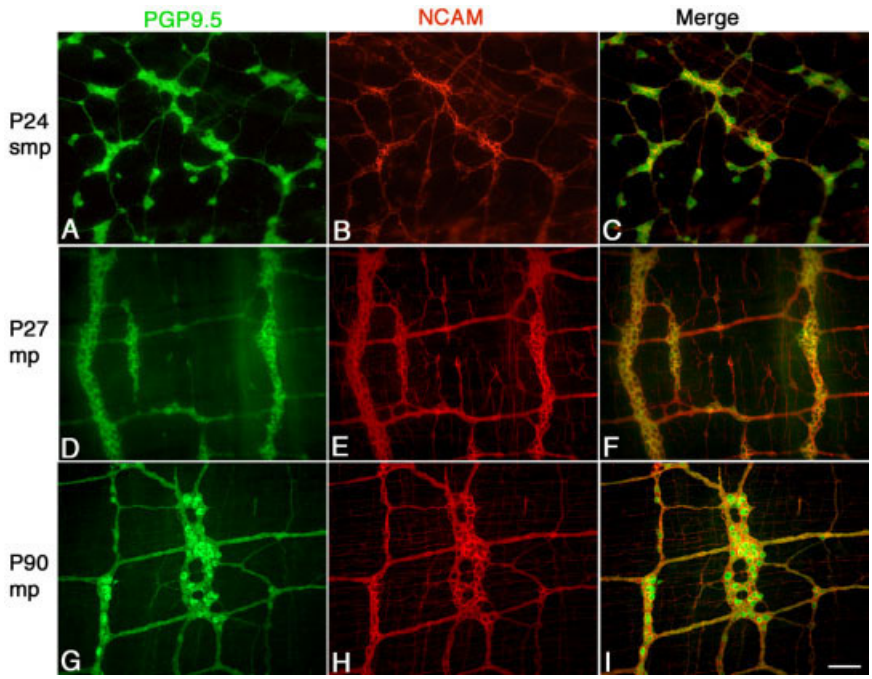

Fig. 8. NCAM continues to be expressed in both plexuses of the adult ENS. Whole mount preparations of the dissected submucosal and myenteric plexuses. **A–C:** P24 Submucosal plexus (smp). **D–F:** P27 Myenteric plexus (mp). **G–I:** P90 Myenteric plexus (mp). A,D,G: Immunoreactivity of PGP9.5; B,E,H: immunoreactivity of NCAM; C,F,I: merged images. Scale bar = 40 μm.

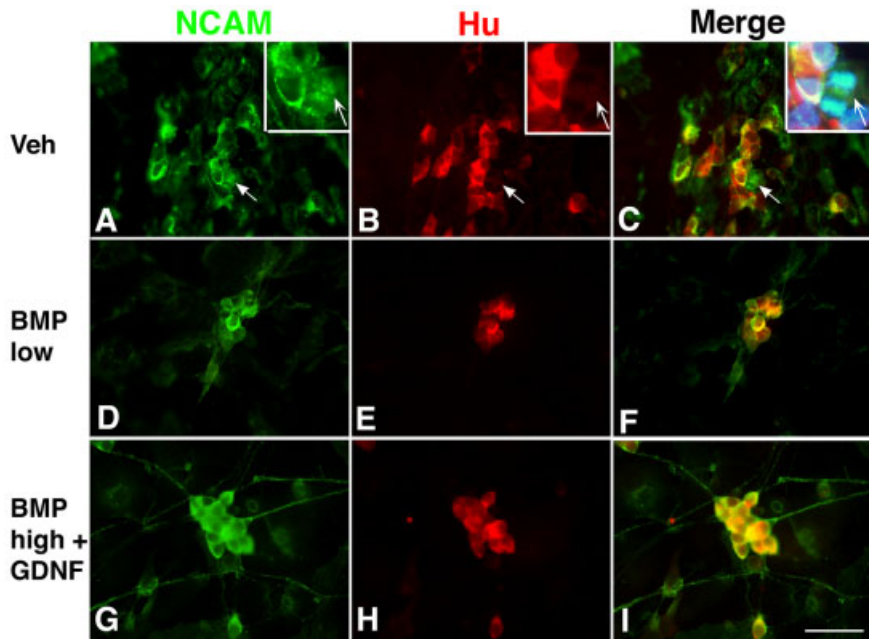

Fig. 9. BMP-4 causes NCAM-expressing neurons developing in vitro from immunoselected enteric crest-derived precursors to cluster. Crest-derived cells were immunoselected from the fetal bowel with antibodies to $p75^{NTR}$ at E12 and cultured for 4 days. **A–C:** Control: cells exposed only to vehicle (Veh). NCAM immunoreactivity (A) is expressed by all neurons identified with antibodies to Hu (B); however, dividing precursor cells (inset) are NCAM-immunoreactive but lack Hu. Note that the neurons are not aggregated in clusters. **D–F:** Exposure to 0.5 ng/ml BMP-4 (BMP low). NCAM-immunoreactive neurons are present in small clusters. **G–I:** Exposure to 50 ng/ml BMP-4 (BMP high) with GDNF to prevent BMP-4-induced loss of neurons. No dividing NCAM-immunoreactive precursors are evident in cultures exposed to either concentration of BMP-4. All NCAM-immunoreactive cells have differentiated as neurons. Larger neuronal clusters are seen. Scale bar = 25 μm.

synaptic plasticity (Phillips et al., 1997; Wood et al., 1997; Brocco et al., 2003). The known plasticity of the ENS might similarly account for the persistence of PST (Lomax et al., 2005). The colonization of the bowel by precursor cells from the neural crest (Rothman et al., 1984; Pomeranz et al., 1991; Young et al., 1998, 1999, 2004b; Anderson et al., 2006) occurs before the maximal expression of STX and PST, which coincides with the initial appearance of terminally differentiated neurons (Rothman et al., 1984) and the rearrangement of chains of crest-derived cells into the precise meshwork of the enteric plexuses (Epstein et al., 1991; Fu et al., 2004; Young et al., 2004b; Tanano et al., 2005). In contrast to intestinal crypts, enteric ganglia are not clones arising from a single stem cell (Rothman et al., 1993). STX and PST are also highly expressed during the time when the developmentally regulated PSA-NCAM is demonstrable in enteric neurons. The evident downregulation of PST and especially STX, however, was found to precede that of PSA-NCAM immunoreactivity. The fact that PSA-NCAM expression declines more gradually than that of STX may reflect the continuing activity of PST and/or a slower rate of turnover of PSA-NCAM than STX and PST transcripts. Interestingly, PSA-NCAM persists in axons of the neuropil and interganglionic connectives after it is lost from nerve cell bodies. The axonal persistence of PSA-NCAM might reflect the continuing outgrowth and remodeling of axonal connections after nerve cell bodies have achieved a stable location. The timing of the expression of STX and PST and both the timing and location of PSA-NCAM are consistent with the postulated role of PSA-NCAM in the organization of neurons and neurites into the mature patterns of the ganglionated plexuses of the ENS.

By E16, the formation of the circular muscle partitions the enteric mesenchyme into distinct internal (mucosal) and external (serosal) compartments. Crest-derived cells colonize the bowel by migrating proximodistally within the outer gut mesenchyme (McKeown et al., 2001). At E16, therefore, enteric neurons are almost exclusively found in the external com-

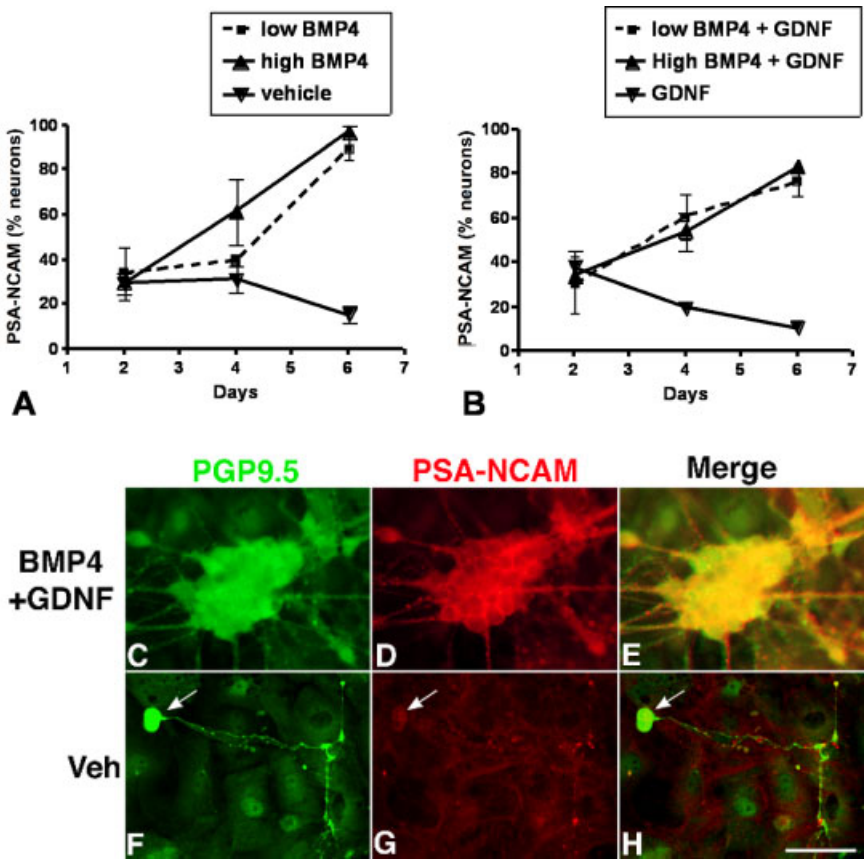

Fig. 10. BMP-4, but not GDNF, promotes the expression of PSA-NCAM in vitro. Crest-derived cells were immunoselected from the fetal bowel with antibodies to $p75^{NTR}$ at E12 and cultured for 6 days. **A:** PSA-NCAM expression as a proportion of total neurons is quantified as a function of time in the presence of vehicle, low, or high concentrations of BMP-4. The proportion of neurons expressing PSA-NCAM increases as a function of time in the presence of either concentration of BMP-4, but fails to do so when cultured in the presence of vehicle. After 6 days exposure to BMP-4, almost all neurons express PSA-NCAM. **B:** PSA-NCAM expression as a proportion of total neurons is quantified as a function of time in the presence of GDNF alone or GDNF plus low or high concentrations of BMP-4. The proportion of neurons expressing PSA-NCAM increases as a function of time when either concentration of BMP-4 is present, but fails to do so when cultured in the presence of GDNF alone. **C–E:** Coincident expression of the immunoreactivity of the neuronal marker, PGP9.5 (C) with that of PSA-NCAM (D) is illustrated. Note that large clusters form when cultures are exposed to BMP-4 + GDNF. **F–H:** Coincident immunoreactivity of PGP9.5 (F) and PSA-NCAM (G) is seen in the scattered neurons that develop in control cultures exposed only to vehicle. Note that both cell body and neurites are PSA-NCAM immunoreactive (E, H). Scale bar = 20 μm.

partment; however, when the submucosal plexus forms, at E18, crest-derived cells have to translocate from the outer to the inner compartment of the bowel (Jiang et al., 2003). This translocation involves a netrin-1-guided migration of crest-derived cells, which express deleted in colorectal cancer (DCC), through the circular muscle. For such a migration to take place, the submucosal neuronal precursors would have to be prevented from adhering to adjacent neurons or glia in primordial myenteric ganglia and to the smooth muscle. Because the developing desmin-immunoreactive circular smooth muscle cells transiently express NCAM, as also do smooth muscle cells in bladder and aorta (Akeson et al., 1988), one might anticipate a homophilic adhesion of NCAM-expressing neuronal precursors within the muscle layer that would interfere with their trans-muscle migration. On the other hand, the NCAM that is transiently expressed by developing circular muscle is polysialylated, as is that of developing neurons. The negatively charged sugar chains of PSA-NCAM are thought to impede homophilic attraction (Rutishauser and Landmesser, 1996; Kiss et al., 2001; Johnson et al., 2005). In fact, it has been shown that a major function of the polysialylation of NCAM is to interfere with NCAM-mediated adhesion (Weinhold et al., 2005). The defect resulting from the genetic deletion of the enzymes that polysialylate NCAM is actually more severe than that observed following the deletion of NCAM and can be rescued by the further deletion of NCAM. The expression of PSA-NCAM in the muscle layer, therefore, might represent a modification that allows, first, the migration of crest-derived cells toward the mucosa to form the submucosal plexus, and, second, the later exploration of the surface of smooth muscle by NCAM-expressing axons seeking correct sites of innervation, such as smooth muscle–associated interstitial cells of Cajal (Ward et al., 2000; Wang et al., 2003).

BMPs were originally postulated to promote polysialylation of NCAM because BMPs-2 and -4 were demonstrated to induce clustering of neurons in vitro (Chalazonitis et al., 2004). For neurons to cluster, the originally scattered cells of the neuronal lineage must be able to move on their substrate to approach one another. The polysialylation of NCAM reduces cell-substrate interactions and thus might make this contemplated migration possible. These ideas were supported by the current observations. BMP-4 was found to increase the formation of PSA-NCAM, an effect that was not shared by GDNF, although GDNF opposed the BMP-4-induced restriction of the expansion of the neuronal population. More neurons in clusters were thus observed when cultures were exposed both to BMP-4 and GDNF than to BMP-4 alone; however, when combined with BMP4, GDNF evidently increased the number of clustered neurons mainly by preserving neurons exposed to BMP-4. The ability of BMP-4 to promote PSA-NCAM expression by cultured neurons correlated with its ability to enhance neuronal clustering. Further experiments were carried out to determine whether the BMP-4-induced increase in PSA-NCAM expression was causally related to the BMP-4-induced increase in neuronal clustering.

ManBut was used to inhibit the formation of PSA-NCAM and ManProp

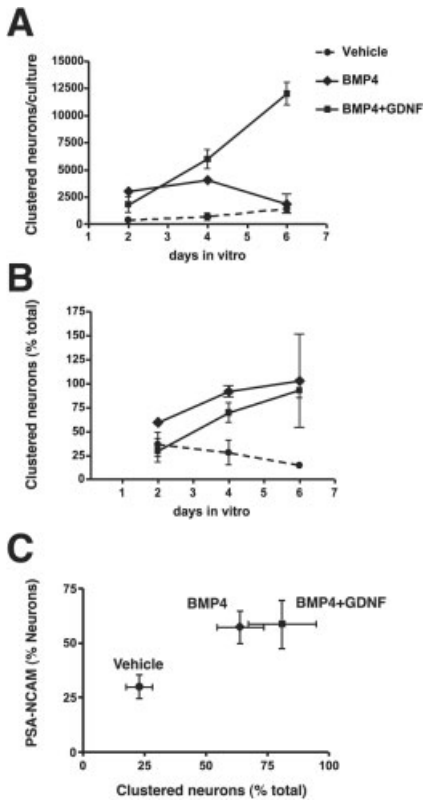

Fig. 11. BMP-4 ± GDNF promotes neuronal expression of PSA-NCAM. and the ability of neurons to form large clusters. Crest-derived cells were immunoselected from the fetal bowel with antibodies to $p75^{NTR}$ at E12 and cultured for 6 days. **A:** The number of clustered neurons surviving in the presence of BMP-4 (50 ng/ml) is enhanced by co- treatment with GDNF (10 ng/ml). **B:** The proportion of neurons aggregating in clusters is increased by BMP-4 but is not further increased by co-treatment with GDNF. **C:** Correlation of increased neuronal PSA-NCAM expression promoted by BMP-4±GDNF is correlated with increased proportions of neurons in clusters.

was employed as a control (Mahal et al., 2001; Charter et al., 2002). In the presence of ManBut, unnatural sialic acids are metabolically generated that effectively terminate the formation of PSA chains on cell surface NCAM. This effect eliminates the anti-adhesive action normally generated by PSA-NCAM. In contrast, the close congener, ManProp, is accepted by polysialyltransferases and permits the extension of poly-N-propanoylsialic acids on NCAM. These extensions do not interfere with the anti-adhesive properties of polysialylated NCAM. Exposure to ManBut, but not to ManProp, was found to inhibit the clustering of neurons induced by BMP-4 in the presence of GDNF. In contrast, neither ManBut nor ManProp affected the total numbers of neurons in the cultures. Because ManBut inhibited BMP-4-induced clustering in vitro, this clustering must depend on BMP-4's ability to promote the polysialylation of NCAM; furthermore, the failure of ManProp to mimic the effect of ManBut implies that the polysialylation of NCAM is required for clustering because of its anti-adhesive properties. Prevention of excessive adhesion of cells to the substrate, permitting them to move, is most likely to be the effect of PSA-NCAM. Evidently, the presence of unnatural poly-N-propanoylsialic acids on NCAM, which preserves anti-adhesion, is compatible with neuronal clustering, as it has also been found to be compatible with neurite extension (Charter et al., 2002).

Although BMPs affect early gut development, and play roles in the regionalization of the bowel (Roberts et al., 1995; Roberts, 2000; De Santa Barbara et al., 2005), their action is not limited to the formation of the primordial gut. BMPs continue to be expressed during the fetal period, when the primordial gut is remodeled into the mature bowel (Chalazonitis et al., 2004). In fact, the developmental regulation of enteric expression of STX and PST, and thus the ability of cells to polysialylate NCAM, mirrors the in vivo developmental regulation of expression of BMP-4 in the gut. BMP-4 expression is detectable at E12, rises at E14, is maintained at a high level through birth, and declines postnatally. BMP2, which stimulates the same receptors as BMP-4 (Cho and Blitz, 1998), is expressed at a high level as early as E12, but it too declines postnatally (Chalazonitis et al., 2004). Enteric neuronal precursors and smooth muscle, moreover, express the BMP receptors IA, IB, and II and display BMP2- and 4-induced phosphorylation and nuclear translocation of Smad-1.

The expression of BMPs and their receptors in the fetal gut is consistent with the idea that BMPs regulate the formation of PSA-NCAM both in neurons and smooth muscle. There is also evidence that the in vitro effect of BMPs on neuronal clustering is relevant to the acquisition of the normal pattern of enteric ganglia in the ENS in vivo. Delivery of noggin (a BMP4-sequestering antagonist) to the developing embryonic chick gut by the in ovo administration of a retroviral vector results in the formation of multiple small ganglia, suggesting an in vivo defect in the clustering of neurons into mature ganglia (Goldstein et al., 2005).

We have demonstrated that cells in neuronal and muscle lineages express NCAM and PSA-NCAM in the fetal rat intestine during the period when the two enteric plexuses are forming. PSA-NCAM and the expression of its biosynthetic enzymes, STX and PST, but not NCAM, are severely downregulated after gangliogenesis has been completed in the postnatal gut. In vitro, BMP-4, in the absence or presence of GDNF, promotes polysialylation of the NCAM that crest-derived neural precursors express. The BMP-4-induced formation of large clusters of neurons is inhibited by the chain terminator, ManBut, which blocks the polysialylation of NCAM, but not by the inactive congener, ManProp. Observations thus support the hypotheses that polysialylation of NCAM is required for the remodeling of chains of neurons into the mature patterns of ganglia and connectives of the enteric plexuses and that BMPs may participate in the sculpting of enteric plexuses by regulating clustering and the polysialylation of NCAM.

EXPERIMENTAL PROCEDURES

Animals

Rats were obtained from a commercial source (Sprague-Dawley, Charles River, Waltham, MA) and killed by CO_2 narcosis. Fetal rats and neonates were decapitated. The Animal Care and Use Committees of Columbia University and Sainte-Justine Hospital Research Center have approved these procedures. The day at which a vaginal plug was found was designated as day 0 of gestation. All animals were housed in cages at a controlled temperature and had free access to food and water.

Real-Time Quantitative RT-PCR

Tissue samples.

Intestines from E12 (n = 15), E14 (n = 16), E18 (n = 6), P1 (n = 3), P8

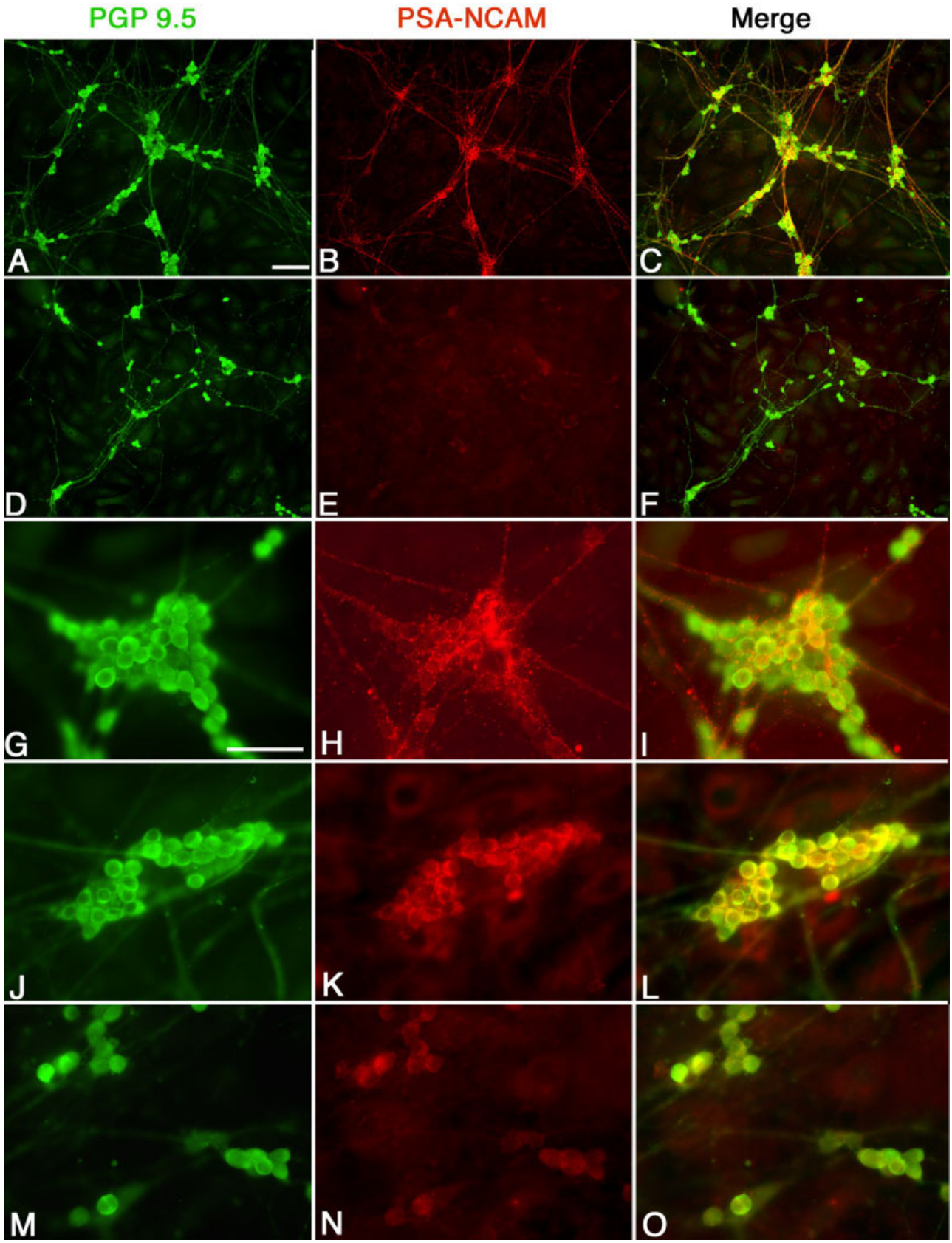

Fig. 12. ManBut, but not its inactive congener, ManProp, inhibits formation of PSA-NCAM and clustering of enteric neurons. Crest-derived cells were immunoselected from fetal rat gut with antibodies to $p75^{NTR}$ and cultured for 5 days. A neuronal marker (PGP.9.5) is demonstrated in the panels at the left (**A,D,G,J,M**), PSA-NCAM immunoreactivity in the center (**B,E,H,K,N**), and the merged images are shown at the right (**C,F,I,L,O**). Low-power fields are illustrated in the upper 6 panels (A–F), in which control conditions (exposure only to BMP-4 and GDNF) (A–C), are compared to cells incubated with BMP-4, GDNF, and ManBut (5.0 mM) (D–F). Higher-power micrographs are illustrated in the bottom 9 panels (G–O). Control conditions (G–I) are compared to ManProp (5.0 mM) (J–L) and ManBut (M–O). Note that ManBut strongly decreases the PSA-NCAM immunoreactivity of neurons and interferes with their clustering (compare D–F [ManBut] with A–C [control] and M–O [ManBut] with G–I [control]). In contrast, ManProp does not interfere substantially either with the PSA-NCAM immunoreactivity of neurons or their clustering (compare J–L [ManProp] with G–I [control] and with M–O [ManBut]). Scale bars = 100 μm.

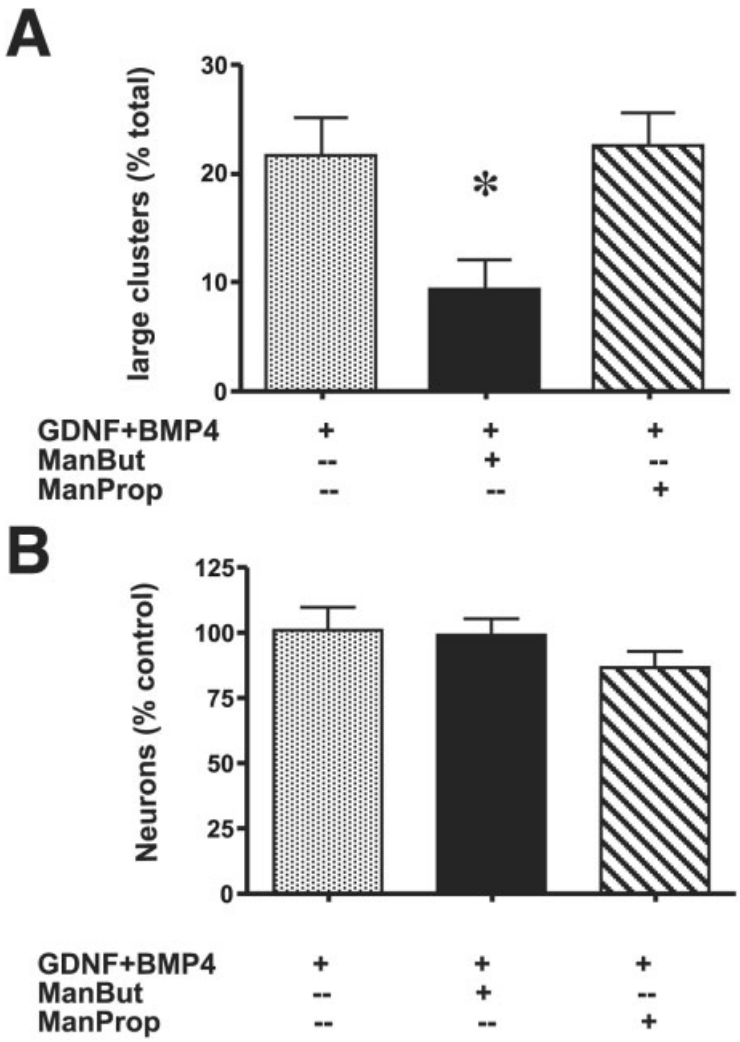

Fig. 13. ManBut, but not ManProp, interferes with neuronal clustering without affecting neuronal survival. **A:** The proportions of neurons in clusters is significantly reduced by ManBut but not by ManProp. **B:** The total number of neurons surviving in vitro in cultures exposed either to ManBut or ManProp is not significantly different from that in cultures grown under control conditions (media supplemented only with BMP4 and GDNF). The presence of the unnatural sialic acid analogs thus does not affect neuronal survival.

(n = 3), P14 (n = 3), P21 (n = 3), P28 (n = 3), and adult (250–300 g) (n = 3) rats were carefully dissected, weighed, frozen, and stored in liquid nitrogen. Brains from E18 fetuses (n = 3) were also removed and examined as a positive control because STX and PST are known to be highly expressed in fetal brain (Phillips et al., 1997).

RNA extraction from tissues.

Total RNA was extracted from the whole intestine using the RNeasy Midi-Kit (Qiagen, Chatsworth, CA) and treated with DNAase (Qiagen). The integrity of extracted RNA was verified by demonstrated distinct bands of 18S and 28S rRNA following electrophoretic separation in 1.5% agarose gels. The samples consistently showed a spectrophotometric 260 nm/280 nm absorption ratio of > 1.9.

Primer design and PCR.

Specific primers for PST and STX genes were designed using Primer3 software (The Whitehead Institute, Boston, MA). Primer specificity was confirmed by a BLAST software–assisted search of a non-redundant nucleotide sequence database (National Library of Medicine, Bethesda, MD) and was tested by using RT-PCR. cDNA encoding β-actin was amplified with the primers: sense: 5′-ACGTTGACATCCGTAAAGACCT-3′ and antisense: 5′-GCAGTAATCTCCTTCTGCATCC-3′ (amplicon length: 100 bp) for 35 cycles (94°C for 45 sec, 60°C for 30 sec, and 72°C for 30 sec). cDNA encoding PST was amplified with the primers: sense 5′-GCAGTTTCAAGCCTGGTGAT-3′ and antisense: 5′-GGTGAAACTTCAGGCAGGAG-3′ (amplicon length: 100 bp) for 35 cycles (94°C for 45 sec, 59°C for 30 sec, and 72°C for 30 sec). cDNA encoding STX was amplified with the primers: sense 5′-GTGGATACCTGCCTTCATGG-3′ and antisense: 5′-CATGGTGCTTCAGGATGAGA-3′ (amplicon length: 77 bp) for 35 cycles (94°C for 45 sec, 58°C for 30 sec, and 72°C for 30 sec). PCR products were separated by agarose (3.0 %) gel electrophoresis. cDNA extracted from E18 fetal brain served as a positive control. Negative controls consisted of omission of reverse transcriptase prior to PCR amplification and the use of distilled water instead of cDNA (Fig. 1).

qPCR.

The levels of transcripts in the rat gastrointestinal tract encoding the polysialyltransferases, PST and STX, were analyzed at different stages of development by real-time quantitative RT-PCR by using a Cepheid Smart Cycler™ system. Total RNA (1 μg) was subjected to reverse transcription by using oligo(dT) primers and SuperScript™ II reverse transcriptase (Invitrogen). Samples were treated with uracyl DNA glycosylase at 50°C for 2 min and then amplified by means of real-time PCR employing a Quantitect™ SYBR® Green PCR kit (Qiagen). Each cycle consisted of three steps: denaturation for 15 s at 94°C, annealing for 30 s at 60°C for β-actin, 59°C for PST, and 58°C for STX, and 30 sec of elongation at 72°C. Data were collected in real-time during the elongation step of each cycle of the 45-cycle reactions. Each cDNA sample was analyzed in triplicate and one sample without cDNA template and one sample without reverse transcriptase were included as negative controls in each experiment. Expression of β-actin was measured in every sample. Melting curve analysis and agarose gel electrophoresis (Fig. 1) confirmed the specificity of the reactions.

The efficiency (Eff = $10^{-(1/\text{slope})}$) of

the PCR reactions was examined by determining the slope of a standard curve over five orders of magnitude in fivefold serial dilutions of cDNA obtained from E18 brains for PST and STX and for β-actin (Rasmussen et al., 2001). The relative quantities of transcripts encoding PST and STX were calculated using the cycle threshold for each sample. β-actin served as an internal control for each sample. The mRNAs encoding PST and STX in the E18 rat brain were used as calibrators. The formula used to calculate the relative values of transcripts encoding PST and STX was: $[(\mathrm{Eff}_{\mathrm{PST\ or\ STX}})^{\text{cycle threshold of PST or STX}} \div (\mathrm{Eff}_{\beta\text{-actin}})^{\text{cycle threshold of }\beta\text{-actin}}] \div (\mathrm{Eff}_{\mathrm{PST\ or\ STX}})^{\text{cycle threshold of PST or STX in E18 brain}}$.

Isolation of Tissue for Immunocytochemistry

E14 fetuses were removed from dams, cleaned and fixed immediately in freshly prepared 4% formaldehyde (from paraformaldehyde) in 0.1 M sodium phosphate buffer (PBS), pH 7.4, for 3 h at room temperature. The gut was dissected prior to fixation from fetuses (E16, E18, and E20), newborn (P1), suckling (P7 and P14), weanling (P24-P26), and adult rats (P45, P60, P90). Immediately after excision, specimens were cleaned of luminal contents material and fixed as described above. Specimens were then cryoprotected by infiltration overnight at 4°C with 30% sucrose in PBS (0.1 M, pH 7.4), embedded in OCT™ (Sakura Finetek 4583) embedding media, and frozen in liquid nitrogen. Sections were cut at 6–8 μm in thickness by using a cryostat-microtome, picked up on slides coated with poly-L-lysine (0.1% in distilled water), and stored at −20°C until used. For whole mount preparations, dissected intestinal segments were opened along the mesenteric border, stretched and pinned flat on Sylgaard™. Specimens were then incubated with PBS (0.1 M, pH 7.4) containing nifedipine 1 μM (Sigma Chemicals, St. Louis, MO) for 30 min and then fixed in Zamboni's fixative for 3 h at room temperature. The mucosa and circular muscular layers were then carefully removed under microscopic control and the completed preparations were immediately processed to demonstrate immunofluorescence.

Immunocytochemistry.

Sections were rinsed with PBS (0.1 M, pH 7.4) containing 0.2% Triton X-100, incubated with 10% normal goat serum (InVitrogen-Gibco BRL Grand Island, NY) for 30 min, and exposed to primary antibodies in a humid chamber for 18–24 h at 4°C. Primary antibodies are listed in Table 1. Negative controls, in which primary antibodies were omitted, were included with each experiment. After incubation with the primary antibodies, sections were rinsed with three changes of PBS (0.1 M, pH 7.4; 10 min/rinse). Polyclonal primary antibodies were located with affinity-purified goat anti-rabbit secondary antibodies that were coupled to Alexa 488 (Molecular Probes, Eugene, OR). Monoclonal antibodies were located with biotinylated affinity-purified goat anti-mouse secondary antibodies (Molecular Probes), which were visualized with streptavidin coupled to Alexa 594 (Molecular Probes).

Quantitative morphometry.

The proportion of neurons that were PSA-NCAM immunoreactive was assessed. The total number of neurons was determined by counting PGP9.5-immunoreactive cells in the fetal and post-natal gut. Cells were counted twice each by two independent observers in 4–6 random fields. Segments of bowel from at least 3 animals were analyzed. Data obtained from each segment of gut were pooled by age. Measurements from the submucosal and myenteric plexuses were quantified separately.

Immunoselection and Culture of Enteric Neuronal Crest–Derived Cells

Immunoselection.

The fetal rat bowel was dissected aseptically at E12 from 20–25 fetuses per experiment. Crest-derived cells were immunoselected from the fetal rat gut with antibodies to the common neurotrophin receptor, $p75^{NTR}$, which is a specific marker for enteric crest-derived cells (Young et al., 1999), at E12 as described previously (Chalazonitis et al., 1998a, 2004). Briefly, the bowel was dissociated with collagenase to yield a single cell suspension, the suspended cells were exposed, sequentially, to antibodies to $p75^{NTR}$, and then to secondary antibodies coupled to magnetic beads; the antibody decorated crest-derived cells were finally selected on a column inserted in the groove of a magnet. This procedure separates enteric crest-derived cells, which are retained on the column by the magnetic field, from the non-crest-derived cells that pass through. The rabbit polyclonal primary antibodies to $p75^{NTR}$ used for immunoselection were donated by Dr. Moses Chao (Skirball Institute, New York University, NY, NY). These antibodies recognize a region of the extracellular domain (amino acids 43–161) and react with $p75^{NTR}$ of both rats and mice (Huber and Chao, 1995). The goat anti-rabbit secondary antibodies coupled to magnetic beads, the columns, and the magnet used for immunoselection were purchased from Miltenyi Biotec Inc. (Auburn, CA).

Tissue culture.

The crest-derived cells were plated at a density of 1.2×10^5 cells/ml onto 12-mm diameter glass cover slips (RESY No. 1001, Germany) that were coated with poly-D-lysine, rat tail collagen, and laminin, as described previously (Chalazonitis et al., 1998a, 2004). All cultures were maintained in a defined medium (Basic Brazeau medium, BBM) (Ziller and Le Douarin, 1983). At the time of plating, the medium was supplemented with 20% horse serum (JRH Biosciences, Lenexa, KS) to promote adherence of cells to the substrate. After 18 hr, this medium was changed to serum-free BBM. When cultures were maintained for longer than 4 days, they were fed with fresh medium on the 4th day. In all experiments, the factors to be studied, which included human recombinant BMP-4 (Genetics Institute Inc. and Wyeth, Cambridge, MA) and GDNF (rat recombinant; R& D Systems, Berkeley, CA), were added to the medium at the time of plating and were present throughout the subsequent culture period. Control cultures were supplemented with the vehicle (0.5% bovine serum albumin in BBM)

TABLE 1. Primary Antibodies

Antigen	Antibody	Dilution	Source	Reference
PGP 9.5	Rabbit polyclonal	1:400	Biogenesis Ltd, Poole, UK	(Wilkinson et al., 1989)
Hu C/D	Biotinylated mouse monoclonal	1:20	Invitrogen-Molecular Probes, Carlsbad, CA	(Wakamatsu and Weston, 1997)
PSA-NCAM	Mouse monoclonal	1:1000	G. Rougon, Luminy, Marseille, France	(Rougon et al., 1986)
NCAM	Mouse monoclonal	1:5	Developmental Hybridoma Bank, University of Iowa, Iowa City, IA	(DiFiglia et al., 1989)
Desmin	Rabbit polyclonal	1:50	Sigma, Saint Louis, MO	(Wu et al., 1999)

in which the growth factors were suspended.

Cultures were maintained for 2, 4, and 6 days. BMP-4 was added at either a low (0.5 ng/ml) or a high (50 ng/ml) concentration, with or without GDNF at 10 ng/ml, a concentration known to promote maximal effect in these cultures (Chalazonitis et al., 1998a, 2004) at the time of plating. The factors or their combination were present throughout the subsequent culture period. At least 3 experiments were performed for each treatment.

To interfere with polysialylation of NCAM, the immunoselected $p75^{NTR}$ crest-derived cells were plated in the presence of BMP-4 (50 ng/ml) with GDNF (10 ng/ml) the optimal treatment to promote neuronal clustering. On the second day after plating, cultures still with BMP-4±GDNF were then exposed for another 4 days to the acetylmannosamine analog ManBut, which specifically blocks polysialylation, to the non-specific analog ManProp, or to vehicle, into which the analogs were dissolved. Two concentrations (2 and 5 mM) of the analogs were used to compare the effectiveness of ManBut vs. ManProp to inhibit PSA-NCAM formation in enteric neurons. ManBut completely inhibited polysialylation both at 2 and 5 mM on both cell bodies and neuritic processes. ManProp at 2 mM failed to inhibit PSA and was also ineffective at 5 mM although polysialylation was sometime absent on neuritic processes. Formation of clusters (>11 neurons) in the presence of BMP-4±GDNF was compared for each analog treatment and for no analog treatment.

Analysis of cultures by immunocytochemistry.

Markers were used that enabled cultured cells to be identified. Species-specific secondary antibodies conjugated to fluorescent probes and procedures used for the immunocytochemical detection of antigens were similar to those described for the *in vivo* experiments. Primary antibodies are listed in Table 1.

Quantitation.

These were done using a Leica DMR microscope with epifluorescence. The total number of cells in each culture and cells specifically identified as neuron (PGP9.5 or Hu-expressing), PSA-NCAM, or NCAM-expressing were counted as previously described (Chalazonitis et al., 1998a,b, 2001, 2004). Counts of the cells expressing PSA-NCAM or NCAM were normalized as a percentage of these cells found in replicate cultures that had only been treated with vehicle or as a proportion of the total cells present in each experimental treatment including vehicle.

Analysis of neuronal clusters.

To compare the size distribution of neuronal clusters with BMP-4±GDNF treatment, 4 sizes of clusters were originally distinguished: small (S) aggregates of 4–10 neurons, medium (M) of11–20 neurons, large (L) of 21–31 neurons, and extra-large (XL) >31 and up to 80 neurons. Because occurrence of the clusters in the S category was the same in vehicle or with BMP-4±GDNF treatment, whereas the distribution of the larger clusters depended on BMP-4 treatment, all other categories (M, L, and XL) were pooled in a single one so that neurons were considered clustered when aggregates included at least 11 neurons. Both the total number of neurons found in clusters and the proportion of the neurons in each culture that were clustered were measured.

Statistics

Means and standard errors were calculated; means were compared by ANOVA, and post hoc comparisons between groups were made when appropriate (Tukey or Bonferroni/Dunn).

ACKNOWLEDGMENTS

The authors thank Michel Simonneau, Geneviève Rougon, Moise Bendayan, and Emile Levy for their support and encouragement and Daniel Roman and Cindy Gauthier for able technical assistance. This work was supported by Sick Kids Foundation grant XG05–026R (C.F.), National Institutes of Health grants DK 58056 (A.C.) and NS15547 (M.D.G.), and grants from Sainte-Justine Hospital Research Centre (C.F.) and Arnold and Mabel Beckman Foundation (K.J.Y., S.G.S.).

REFERENCES

Akeson RA, Wujek JR, Roe S, Warren SL, Small SJ. 1988. Smooth muscle cells transiently express NCAM. Brain Res 464: 107–120.

Akitaya T, Bronner-Fraser M. 1992. Expression of cell adhesion molecules during initiation and cessation of neural crest cell migration. Dev Dyn 194:12–20.

Anderson RB, Stewart AL, Young HM. 2006. Phenotypes of neural-crest-derived cells in vagal and sacral pathways. Cell Tissue Res 323:11–25.

Angata K, Nakayama J, Fredette B, Chong K, Ranscht B, Fukuda M. 1997. Human STX polysialyltransferase forms the embryonic form of the neural cell adhesion

molecule. Tissue-specific expression, neurite outgrowth, and chromosomal localization in comparison with another polysialyltransferase, PST. J Biol Chem 272:7182–7190.

Araki T, Milbrandt J. 2000. Ninjurin2, a novel homophilic adhesion molecule, is expressed in mature sensory and enteric neurons and promotes neurite outgrowth. J Neurosci 20:187–195.

Baetge G, Pintar JE, Gershon MD. 1990. Transiently catecholaminergic (TC) cells in the bowel of the fetal rat: precursors of noncatecholaminergic enteric neurons. Dev Biol 141:353–380.

Bally-Cuif L, Goridis C, Santoni MJ. 1993. The mouse NCAM gene displays a biphasic expression pattern during neural tube development. Development 117:543–552.

Bonfanti L, Olive S, Poulain DA, Theodosis DT. 1992. Mapping of the distribution of polysialylated neural cell adhesion molecule throughout the central nervous system of the adult rat: an immunohistochemical study. Neuroscience 49:419–436.

Brocco M, Pollevick GD, Frasch AC. 2003. Differential regulation of polysialyltransferase expression during hippocampus development: Implications for neuronal survival. J Neurosci Res 74:744–753.

Bruses JL, Rutishauser U. 2001. Roles, regulation, and mechanism of polysialic acid function during neural development. Biochimie 83:635–643.

Burns AJ, Le Douarin NM. 1998. The sacral crest contributes neurons and glia to the post-umbilical gut: spatiotemporal analysis of the development of the enteric nervous system. Development 125: 4335–4347.

Chalazonitis A. 2004. Neurotrophin-3 in the development of the enteric nervous system. Prog Brain Res 146:243–263.

Chalazonitis A, Rothman TP, Chen J, Gershon MD. 1998a. Age-dependent differences in the effects of GDNF and NT-3 on the development of neurons and glia from neural crest-derived precursors immunoselected from the fetal rat gut: expression of GFRalpha-1 in vitro and in vivo. Dev Biol 204:385–406.

Chalazonitis A, Rothman TP, Chen J, Vinson EN, MacLennan AJ, Gershon MD. 1998b. Promotion of the development of enteric neurons and glia by neuropoietic cytokines: interactions with neurotrophin-3. Dev Biol 198:343–365.

Chalazonitis A, Pham TD, Rothman TP, DiStefano PS, Bothwell M, Blair-Flynn J, Tessarollo L, Gershon MD. 2001. Neurotrophin-3 is required for the survival-differentiation of subsets of developing enteric neurons. J Neurosci 21:5620–5636.

Chalazonitis A, D'Autreaux F, Guha U, Pham TD, Faure C, Chen JJ, Roman D, Kan L, Rothman TP, Kessler JA, Gershon MD. 2004. Bone morphogenetic protein-2 and -4 limit the number of enteric neurons but promote development of a TrkC-expressing neurotrophin-3-dependent subset. J Neurosci 24:4266–4282.

Charter NW, Mahal LK, Koshland DE, Jr., Bertozzi CR. 2002. Differential effects of unnatural sialic acids on the polysialylation of the neural cell adhesion molecule and neuronal behavior. J Biol Chem 277: 9255–9261.

Cho KW, Blitz IL. 1998. BMPs, Smads and metalloproteases: extracellular and intracellular modes of negative regulation. Curr Opin Gen Dev 8:443–449.

Crossin KL, Krushel LA. 2000. Cellular signaling by neural cell adhesion molecules of the immunoglobulin superfamily. Dev Dyn 218:260–279.

De Santa Barbara P, Williams J, Goldstein AM, Doyle AM, Nielsen C, Winfield S, Faure S, Roberts DJ. 2005. Bone morphogenetic protein signaling pathway plays multiple roles during gastrointestinal tract development. Dev Dyn 234:312–322.

DiFiglia M, Marshall P, Covault J, Yamamoto M. 1989. Ultrastructural localization of molecular subtypes of immunoreactive neural cell adhesion molecule (NCAM) in the adult rodent striatum. J Neurosci 9:4158–4168.

Durbec PL, Larsson-Blomberg LB, Schuchardt A, Costantini F, Pachnis V. 1996. Common origin and developmental dependence on c-ret of subsets of enteric and sympathetic neuroblasts. Development 122:349–358.

Eckhardt M, Bukalo O, Chazal G, Wang L, Goridis C, Schachner M, Gerardy-Schahn R, Cremer H, Dityatev A. 2000. Mice deficient in the polysialyltransferase ST8SiaIV/PST-1 allow discrimination of the roles of neural cell adhesion molecule protein and polysialic acid in neural development and synaptic plasticity. J Neurosci 20:5234–5244.

Enomoto H, Araki T, Jackman A, Heuckeroth RO, Snider WD, Johnson EM, Jr., Milbrandt J. 1998. GFR alpha1-deficient mice have deficits in the enteric nervous system and kidneys. Neuron 21:317–324.

Epstein M, Poulsen KT, Thiboldeaux R. 1991. Formation of ganglia in the gut of the chick embryo. J Comp Neurol 307: 189–199.

Faure C, Rhéaume C, Chalazonitis A, Gershon MD. 2003. Expression of polysialylated neural cell adhesion molecule (PSA-NCAM) in the developing and mature rat enteric nervous system (ENS): relationship to neuronal differentiation and plasticity. In: Enteric Nervous System Conference. Banff, Alberta. 9–13 July 2003. Neurogastroenterol Motil 15:85.

Fu M, Tam PK, Sham MH, Lui VC. 2004. Embryonic development of the ganglion plexuses and the concentric layer structure of human gut: a topographical study. Anat Embryol (Berl) 208:33–41.

Furness JB. 2000. Types of neurons in the enteric nervous system. J Auton Nerv Syst 81:87–96.

Furness JB, Costa M. 1987. The enteric nervous system. New York: Churchill Livingstone.

Gershon MD. 2000. Functional anatomy of the enteric nervous system: a developmental perspective relevant to the pathogenesis of Hirschsprung's disease. In: Holschneider AM, Puri P, editors. Hirschsprung's disease and allied disorders. Amsterdam, The Netherlands: Harwood Academic Publishers. p 19–58.

Gershon MD, Kirchgessner AL, Wade PR. 1994. Functional anatomy of the enteric nervous system. In: Johnson LR, Alpers DH, Jacobson ED, Walsh JH, editors. Physiology of the gastrointestinal tract, 3rd ed. New York: Raven Press. p 381–422.

Gianino S, Grider JR, Cresswell J, Enomoto H, Heuckeroth RO. 2003. GDNF availability determines enteric neuron number by controlling precursor proliferation. Development 130:2187–2198.

Glass JD, Lee W, Shen H, Watanabe M. 1994. Expression of immunoreactive polysialylated neural cell adhesion molecule in the suprachiasmatic nucleus. Neuroendocrinology 60:87–95.

Goldstein AM, Brewer KC, Doyle AM, Nagy N, Roberts DJ. 2005. BMP signaling is necessary for neural crest cell migration and ganglion formation in the enteric nervous system. Mech Dev 122:821–833.

Heuckeroth RO, Lampe PA, Johnson EM, Milbrandt J. 1998. Neurturin and GDNF promote proliferation and survival of enteric neuron and glial progenitors in vitro. Dev Biol 200:116–129.

Huber LJ, Chao MV. 1995. A potential interaction of p75 and trkA NGF receptors revealed by affinity crosslinking and immunoprecipitation. J Neurosci Res 40: 557–563.

Jiang Y, Liu M-t, Gershon MD. 2003. Netrins and DCC in the guidance of migrating neural crest-derived cells in the developing bowel and pancreas. Developmental Biology 258:364–384.

Johnson CP, Fujimoto I, Rutishauser U, Leckband DE. 2005. Direct evidence that neural cell adhesion molecule (NCAM) polysialylation increases intermembrane repulsion and abrogates adhesion. J Biol Chem 280:137–145.

Kapur RP. 2000. Colonization of the murine hindgut by sacral crest-derived neural precursors: experimental support for an evolutionarily conserved model. Dev Biol 227:146–155.

Kiss JZ, Troncoso E, Djebbara Z, Vutskits L, Muller D. 2001. The role of neural cell adhesion molecules in plasticity and repair. Brain Res Brain Res Rev 36:175–184.

Kojima N, Kono M, Yoshida Y, Tachida Y, Nakafuku M, Tsuji S. 1996. Biosynthesis and expression of polysialic acid on the neural cell adhesion molecule is predominantly directed by ST8Sia II/STX during in vitro neuronal differentiation. J Biol Chem 271:22058–22062.

Le Douarin NM, Teillet MA. 1973. The migration of neural crest cells to the wall of the digestive tract in avian embryo. J Embryol Exp Morphol 30:31–48.

Le Douarin NM, Teillet MA. 1974. Experimental analysis of the migration and differentiation of neuroblasts of the autonomic nervous system and of neurectodermal mesenchymal derivatives, using a biological cell marking technique. Dev. Biol. 41:162–184.

Lois C, Garcia-Verdugo JM, Alvarez-Buylla A. 1996. Chain migration of neuronal precursors. Science 271:978–981.

Lomax AE, Fernandez E, Sharkey KA. 2005. Plasticity of the enteric nervous system during intestinal inflammation. Neurogastroenterol Motil 17:4–15.

Mahal LK, Charter NW, Angata K, Fukuda M, Koshland DE Jr, Bertozzi CR. 2001. A small-molecule modulator of poly-alpha 2,8-sialic acid expression on cultured neurons and tumor cells. Science 294:380–381.

McKeown SJ, Chow CW, Young HM. 2001. Development of the submucous plexus in the large intestine of the mouse. Cell Tissue Res 303:301–305.

Mirsky R, Jessen KR, Schachner M, Goridis C. 1986. Distribution of the adhesion molecules N-CAM and L1 on peripheral neurons and glia in adult rats. J Neurocytol 15:799–815.

Moore MW, Klein RD, Fariñas I, Sauer H, Armanini M, Phillips H, L.F. R, Ryan AM, Carver-Moore K, Rosenthal A. 1996. Renal and neuronal abnormalities in mice lacking GDNF. Nature 382:76–79.

Nakayama J, Fukuda M. 1996. A human polysialyltransferase directs in vitro synthesis of polysialic acid. J Biol Chem 271: 1829-1832.

Nakayama J, Fukuda MN, Fredette B, Ranscht B, Fukuda M. 1995. Expression cloning of a human polysialyltransferase that forms the polysialylated neural cell adhesion molecule present in embryonic brain. Proc Natl Acad Sci USA 92:7031–7035.

Nakayama J, Angata K, Ong E, Katsuyama T, Fukuda M. 1998. Polysialic acid, a unique glycan that is developmentally regulated by two polysialyltransferases, PST and STX, in the central nervous system: from biosynthesis to function. Pathol Int 48:665–677.

Natarajan D, Marcos-Gutierrez C, Pachnis V, de Graaff E. 2002. Requirement of signalling by receptor tyrosine kinase RET for the directed migration of enteric nervous system progenitor cells during mammalian embryogenesis. Development 129:5151–5160.

Newgreen D, Young HM. 2002. Enteric nervous system: development and developmental disturbances: part 1. Pediatr Dev Pathol 5:224–247.

Newgreen DF, Hartley L. 1995. Extracellular matrix and adhesive molecules in the early development of the gut and its innervation in normal and spotting lethal rat embryos. Acta Anat (Basel) 154:243–260.

Paratcha G, Ledda F, Ibanez CF. 2003. The neural cell adhesion molecule NCAM is an alternative signaling receptor for GDNF family ligands. Cell 113:867–879.

Phillips GR, Krushel LA, Crossin KL. 1997. Developmental expression of two rat sialyltransferases that modify the neural cell adhesion molecule, N-CAM. Brain Res Dev Brain Res 102:143–155.

Pichel JG, Shen L, Sheng HZ, Granholm A-C, Drago J, Grinberg A, Lee EJ, Huang SB, Saarma M, Hoffer BJ, Sariola H, Westphal H. 1996. Defects in enteric innervation and kidney development in mice lacking GDNF. Nature 382:73–76.

Pomeranz HD, Rothman TP, Gershon MD. 1991. Colonization of the post-umbilical bowel by cells derived from the sacral neural crest: direct tracing of cell migration using an intercalating probe and a replication-deficient retrovirus. Development 111:647–655.

Rasmussen R. 2001. Quantification on the LightCycler. In: Meuer S, Wittwer C, Nakagawara K, editors. Rapid cycle real-time PCR, methods and applications. Heidelberg: Springer Press. pp 21–34.

Roberts DJ. 2000. Molecular mechanisms of development of the gastrointestinal tract. Dev Dyn 219:109–120.

Roberts DJ, Johnson RL, Burke AC, Nelson CE, Morgan BA, Tabin C. 1995. Sonic hedgehog is an endodermal signal inducing *Bmp-4* and *Hox* genes during induction and regionalization of the chick hindgut. Development 121:3163–3174.

Romanska HM, Bishop AE, Moscoso G, Walsh FS, Spitz L, Brereton RJ, Polak JM. 1996. Neural cell adhesion molecule (NCAM) expression in nerves and muscle of developing human large bowel. J Pediatr Gastroenterol Nutr 22:351–358.

Rothman TP, Goldowitz D, Gershon MD. 1993. Inhibition of migration of neural crest-derived cells by the abnormal mesenchyme of the presumptive aganglionic bowel of *ls/ls* mice: analysis with aggregation and interspecies chimeras. Dev Biol 159:559-573.

Rothman TP, Nilaver G, Gershon MD. 1984. Colonization of the developing murine enteric nervous system and subsequent phenotypic expression by the precursors of peptidergic neurons. J Comp Neurol 225:13–23.

Rougon G, Hobert O. 2003. New insights into the diversity and function of neuronal immunoglobulin superfamily molecules. Annu Rev Neurosci 26:207–238.

Rougon G, Dubois C, Buckley N, Magnani JL, Zollinger W. 1986. A monoclonal antibody against meningococcus group B polysaccharides distinguishes embryonic from adult N-CAM. J Cell Biol 103:2429–2437.

Rutishauser U, Landmesser L. 1996. Polysialic acid in the vertebrate nervous system: a promoter of plasticity in cell-cell interactions. Trends Neurosci 19:422–427.

Sánchez M, Silos-Santiago I, Frisén J, He B, Lira S, Barbacid M. 1996. Renal agenesis and the absence of enteric neurons in mice lacking GDNF. Nature 382:70–73.

Schuchardt A, D'Agati V, Larsson-Blomberg L, Costantini F, Pachnis V. 1994. Defects in the kidney and enteric nervous system of mice lacking the tyrosine kinase receptor Ret. Nature 367:380–383.

Seki T, Arai Y. 1993. Distribution and possible roles of the highly polysialylated neural cell adhesion molecule (NCAM-H) in the developing and adult central nervous system. Neurosci Res 17:265–290.

Serbedzija GN, Burgan S, Fraser SE, Bronner-Fraser M. 1991. Vital dye labeling demonstrates a sacral neural crest contribution to the enteric nervous system of chick and mouse embryos. Development 111:857–866.

Tanano A, Hamada Y, Takamido S, Kataoka Y, Watanabe J, Kamiyama Y, Yamada H. 2005. Structural development of PGP9.5-immunopositive myenteric plexus in embryonic rats. Anat Embryol (Berl) 209:341–348.

Wakamatsu Y, Weston JA. 1997. Sequential expression and role of Hu RNA-binding proteins during neurogenesis. Development 124:3449–3460.

Wang XY, Paterson C, Huizinga JD. 2003. Cholinergic and nitrergic innervation of ICC-DMP and ICC-IM in the human small intestine. Neurogastroenterol Motil 15:531–543.

Ward SM, Beckett EA, Wang X, Baker F, Khoyi M, Sanders KM. 2000. Interstitial cells of Cajal mediate cholinergic neurotransmission from enteric motor neurons. J Neurosci 20:1393–1403.

Weinhold B, Seidenfaden R, Rockle I, Muhlenhoff M, Schertzinger F, Conzelmann S, Marth JD, Gerardy-Schahn R, Hildebrandt H. 2005. Genetic ablation of polysialic acid causes severe neurodevelopmental defects rescued by deletion of the neural cell adhesion molecule. J Biol Chem 280:42971–42977.

Wilkinson KD, Lee KM, Deshpande S, Duerksen-Hughes P, Boss JM, Pohl J. 1989. The neuron-specific protein PGP 9.5 is a ubiquitin carboxyl-terminal hydrolase. Science 246:670–673.

Wood GK, Liang JJ, Flores G, Ahmad S, Quirion R, Srivastava LK. 1997. Cloning and in situ hybridization analysis of the expression of polysialyltransferase mRNA in the developing and adult rat brain. Brain Res Mol Brain Res 51:69–81.

Wu JJ, Chen JX, Rothman TP, Gershon MD. 1999. Inhibition of in vitro enteric neuronal development by endothelin-3: mediation by endothelin B receptors. Development 126:1161–1173.

Young H, Hearn CJ, Ciampoli D, Southwell BR, Brunet JF, Newgreen DF. 1998. A single rostrocaudal colonization of the rodent intestine by enteric neuron precursors is revealed by the expression of Phox2B, Ret, and p75 and by explants grown under the kidney capsule or in organ culture. Dev. Biol. 202:67–84.

Young HM, Anderson RB, Anderson CR. 2004a. Guidance cues involved in the development of the peripheral autonomic nervous system. Auton Neurosci 112:1–14.

Young HM, Bergner AJ, Anderson RB, Enomoto H, Milbrandt J, Newgreen DF, Whitington PM. 2004b. Dynamics of neural crest-derived cell migration in the embryonic mouse gut. Dev Biol 270:455–473.

Young HM, Ciampoli D, Hsuan J, Canty AJ. 1999. Expression of Ret-, p75(NTR)-, Phox2a-, Phox2b-, and tyrosine hydroxylase-immunoreactivity by undifferentiated neural crest-derived cells and different classes of enteric neurons in the embryonic mouse gut. Dev Dyn 216:137–152.

Young HM, Hearn CJ, Farlie PG, Canty AJ, Thomas PQ, Newgreen DF. 2001. GDNF is a chemoattractant for enteric neural cells. Dev Biol 229:503–516.

Ziller C, Le Douarin NM. 1983. Neuronal differentiation in cultured neural crest cells: the effect of serum on neurite outgrowth. Birth Defects Orig Artic Ser 19:251–261.